Journal of Hydrology 529 (2015) 94–105

Contents lists available at ScienceDirect

Journal of Hydrology

journal homepage: www.elsevier.com/locate/jhydrol

Implication of remotely sensed data to incorporate land cover effect into a linear reservoir-based rainfall–runoff model

Vahid Nourani [a,*], Ahmad Fakheri Fard [b], Faegheh Niazi [b], Hoshin V. Gupta [c], David C. Goodrich [d], Khalil Valizadeh Kamran [e]

[a] Department of Water Resources Engineering, Faculty of Civil Engineering, University of Tabriz, Tabriz, Iran
[b] Department of Water Engineering, Faculty of Agriculture, University of Tabriz, Tabriz, Iran
[c] Department of Hydrology and Water Resources, University of Arizona, Tucson, AZ, USA
[d] USDA Agricultural Research Service, Southwest Watershed Research Center, Tucson, AZ, USA
[e] Department of Remote Sensing and GIS, Faculty of Geography and Planning, University of Tabriz, Tabriz, Iran

ARTICLE INFO

Article history:
Received 18 March 2015
Received in revised form 16 June 2015
Accepted 16 July 2015
Available online 21 July 2015
This manuscript was handled by Corrado Corradini, Editor-in-Chief, with the assistance of Okke Batelaan, Associate Editor

Keywords:
Geomorphology based rainfall–runoff modeling
Remote sensing
NDVI
Land use/cover
Linear reservoir
La Terraza watershed

SUMMARY

This study investigates the effect of land use on the Geomorphological Cascade of Unequal linear Reservoirs (GCUR) model using the Normalized Difference Vegetation Index (NDVI) derived from remotely sensed data as a measure of land use. The proposed modeling has two important aspects: it considers the effects of both watershed geomorphology and land use/cover, and it requires only one parameter to be estimated through the use of observed rainfall–runoff data. Geographic Information System (GIS) tools are employed to determine the parameters associated with watershed geomorphology, and the Vegetation Index parameter is extracted from historical Landsat images.

The modeling is applied via three formulations to a watershed located in Southeastern Arizona, which consists of two gaged sub-watersheds with different land uses. The results show that while all of the formulations generate forecasts of the basin outlet hydrographs with acceptable accuracy, only the two formulations that consider the effects of land cover (using NDVI) provide acceptable results at the outlets of the sub-watersheds.

© 2015 Elsevier B.V. All rights reserved.

1. Introduction

1.1. Background

The influence of urbanization, as one important form of land use and land cover changes, on runoff and floods within watersheds has been a major topic of research during the past few decades. Hydrologic response of a watershed indicates its condition, and the overall function of the watershed might be affected by land cover changes (Miller et al., 2002). Urbanization affects the hydrologic processes of a watershed by replacing vegetated land cover with paved surfaces, and by changing the natural drainage network via inclusion of artificial structures. This can have a substantial impact on the hydrological reaction of a watershed to the input, potentially resulting in quick response (Huang et al., 2008), greater river flow volume (Hawley and Bledsoe, 2011), higher recurrence of floods (Hollis, 1975; Braud et al., 2013), and decreased base-flow, and reduced sub-surface recharge (Simmons and Reynolds, 1982).

The direct runoff hydrograph of a watershed indicates the characteristics of the effective rainfall hyetograph and the land surface features which control the runoff generation and overland flow processes. Due to the complexity of the rainfall–runoff relationship, conceptual rainfall–runoff models are commonly employed to analyze and simulate this relationship. Such models are popular because in these models, the transformation of rainfall to runoff is mimicked relying on a simple explanation of physical processes to suggest an integration of ease of development and use, and providing acceptable outcome and transparency (de Vos et al., 2010). In particular, conceptual unit hydrograph (UH)-based models, derived from linear systems theory, have been used to investigate the effects of urbanization on rainfall–runoff process (e.g. see Kang et al., 1998; Cheng and Wang, 2002; Huang et al., 2008). The Nash model, consisting of a cascade of identical linear reservoirs, is

* Corresponding author. Tel.: +98 914 403 0332.
E-mail address: vnourani@yahoo.com (V. Nourani).

http://dx.doi.org/10.1016/j.jhydrol.2015.07.020
0022-1694/© 2015 Elsevier B.V. All rights reserved.

among the more popular such models as it gives an explicit formula for the Instantaneous Unit Hydrograph (IUH) (Nash, 1957).

To develop the next generation of the IUHs, the overall response of a watershed was characterized as a function of geomorphologic properties of the watershed. The first remarkable suggestion in this field as a geomorphologic IUH (GIUH) was proposed by Rodríguez-Iturbe and Valdés (1979). On the basis of conceptual framework of the Nash's IUH, Chaoqun et al. (2008) proposed a methodology for determining how the mean residence time (storage coefficient) of each reservoir is related to the topography of the watershed. Agirre et al. (2005) and López et al. (2005) introduced unit hydrograph models considering watershed geomorphology and linear reservoirs, applying a fixed calibrated mean residence time for all reservoirs; the watershed morphology was employed just for the determination of linear reservoirs without any consideration of the sub-basin physiographical properties. López et al. (2012) compared the formerly developed one-parameter IUH model with four other IUH models. Nourani and Mano (2007) used TOPMODEL and the kinematic wave approach wherein all model parameters, except one, were linked to the geomorphologic properties. Nourani et al. (2009) developed three linear reservoir based models and compared the results with classic Nash and SCS (Soil Conservation Service) models; their results showed that although the developed models could lead to better performance in rainfall–runoff modeling, the semi-distributed routing ability can help the model to produce more reliable results in compared with fully lumped models. More recently, Saeidifarzad et al. (2014) presented a multi-site calibration for two geomorphologic linear reservoir models via two calibration strategies.

Unlike lumped models, semi-distributed geomorphologic models need large amount of spatial information in which a combination of remote sensing, Geographic Information Systems (GIS), and simulation modeling can provide and manage spatial data at landscape to global scales (Pickup, 1995). NASA Earth Observing System efforts offer exciting possibilities to couple hydrologic models and directly incorporate remotely sensed data (Goodrich and Woolhiser, 1991). Remote sensing provides various hydro-geomorphologic measurements of variables which are used in hydrologic and environmental modeling. The digital remote sensing data are typically in pixel format and this makes them suitable to be merged with GIS. Estimation of vegetation conditions by remotely sensed data has also been successful (Qi et al., 2000). The classified land cover maps obtained from remote sensing data are used as input parameters of a wide range of hydro-environmental models (Miller et al., 2007); therefore as an implication, a watershed's land use/cover changes can be detected and monitored by remotely sensed data.

Changes in land use include surface characteristics such as impervious cover and vegetation, which can affect the resulting runoff index and speed of runoff travel in the drainage area (Ferguson, 1998). Research into the impacts of vegetation change on water budget at watershed scale has been subject of extensive observation and modeling (e.g., McGulloch and Robinson, 1993). There is evidence that changes in land use can significantly influence the hydrological behavior of a basin (Jones and Grant, 1996).

Coincident with the progress in remote sensing and GIS, it has been shown that in hydrological modeling, the use of remote sensing data to detect spatially consistent values for imperviousness is more appropriate and efficient (e.g., Chormanski et al., 2008; Canters et al., 2011). Widely available earth observation data such as Landsat images for detecting land cover changes via Normalized Difference Vegetation Index (NDVI) have demonstrated to be very beneficial for the successful evaluation, monitoring and depiction of landscape situations in many areas (Ma and Frank, 2006). NDVI is functionally correlated with the leaf area index (LAI) and vegetation coverage (Baret and Guyot, 1991); the higher the NDVI, the larger the LAI, and the higher the vegetation coverage. Therefore, NDVI can reflect the growth status of surface vegetation and act as an effective index for monitoring vegetation variations (Tucker et al., 1985). There are some studies which considered the effect of vegetation cover using NDVI on different hydrologic properties such as inflow into the reservoirs (Wang et al., 2012), runoff coefficient (Sriwongsiatnon and Taesombat, 2011), runoff and sediment yield (Braud et al., 2001), rainfall and temperature (Wang et al., 2003; Udelhoven et al., 2009) and evapotranspiration (Sun et al., 2004); but to the best of authors' knowledge, incorporating NDVI vegetation cover into conceptual rainfall–runoff models has rarely (if ever) been done. In some of the formerly proposed IUH models (e.g., Agirre et al., 2005; Chaoqun et al. (2008); Huang et al., 2008; Nourani et al., 2009; Cheng and Wang, 2002; López et al., 2012) the effects of land cover variation over the watershed have not been incorporated into the model formulation, explicitly. Therefore, such models although may appropriately predict the output hydrographs in watersheds with roughly uniform land uses; they will be unable to reliably estimate interior sub-watershed's outlet hydrographs in a watershed with extremely heterogeneous land uses.

1.2. Scope

This study proposes an integration of remote sensing and GIS tools for monitoring the land-cover and urbanization condition of a watershed to determine the effects of changes on the watershed responses predicted from a geomorphology-based semi-distributed rainfall–runoff model.

The approach is used to investigate land cover impacts for a small, well instrumented pair of watershed in the city of Sierra Vista, Cochise County, Southeastern Arizona through three steps of: (i) Determining the land cover changes in two sub-watersheds of study area with different land uses using the Landsat 4–5 TM (Thematic Mapper) satellite images, (ii) Developing a Geomorphological Cascade of Unequal linear Reservoirs (GCUR) model integrated with the NDVIs of different land cover types, and (iii) Demonstrating model performance and suitability through three different formulations using available hydro-geomorphological data.

In the next sections of the paper, the study area and data sources including field measurements and satellite data, and the methodology for remote sensing analysis and the concept of NDVI are described. Subsequent sections present the hydrologic model considering three different formulations, and the performance criteria. The results obtained via the proposed modeling framework are then presented and discussed, followed by concluding remarks.

2. Study area and data

2.1. Study area

The study watershed consists of a 32-ha mesquite grassland and a 13-ha residential area (mentioned respectively as the '*grassland*' and '*urban*' sub-watersheds, in this study) in the City of Sierra Vista, Cochise County, in Southeastern Arizona (Fig. 1). The study area is at ~1300 m elevation, in the transition zone between the Sonoran Desert to the west and the Chihuahuan Desert to the south and east. Average annual precipitation is roughly 370 mm with approximately 65% originating from localized convective air mass thunderstorms from June to September during the Mexican monsoon, roughly 5% from late summer tropical depression and the remainder from low-intensity frontal systems during the winter (Goodrich et al., 2008). The elevation

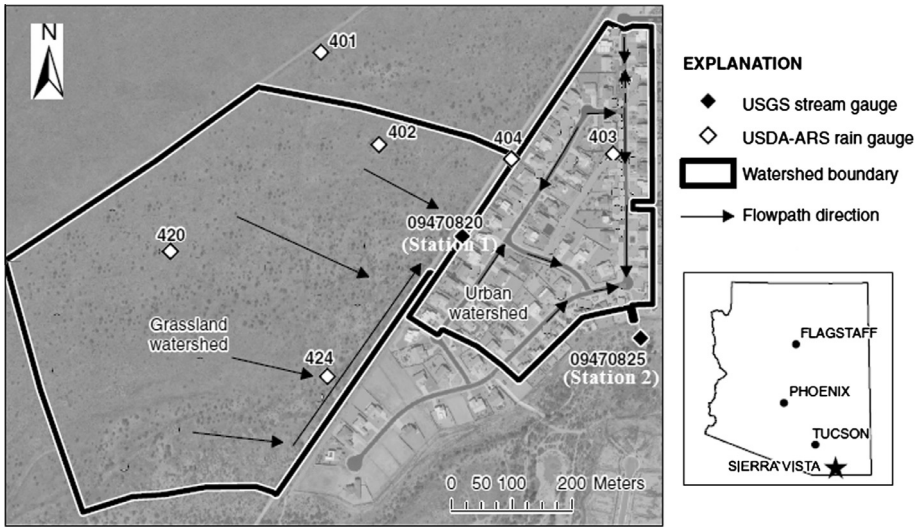

Fig. 1. Study area map showing gauge locations and watershed boundaries. (background image courtesy USGS earth resources observation and science center, from Kennedy et al. (2013).

differences between the highest point in the grassland sub-watershed and its gaged outlet, and the outlet of the grassland sub-watershed and the urbanized watershed's outlet are 25 m and 6 m, respectively. Local ground slope varies between 1% and 10%. Urbanization was occurred mainly between 2001 and 2005 and is typical of most tract-style housing in the Southwestern United States. Storms are drained through the streets, except a 1.3 ha area in the northern urbanized part that drains to the watershed outlet via a 61-cm corrugated pipe. Vegetation in the developed sub-watershed is premature, with a few areas of canopy cover. All pervious surfaces are covered with 2- to 4-cm-diameter gravel mulch, about 10-cm deep, excluding a few small irrigated turf areas (Kennedy et al., 2013).

Overland flow from the grassland sub-watershed drains via a gauged v-notch weir into the urbanized sub-watershed (USGS 09470820 La Terraza Inflow near Sierra Vista, AZ). Runoff from both the grassland and urbanized sub-watersheds is then measured using a v-notch weir at the outlet of the urbanized sub-watershed (USGS 09470825 La Terraza Outflow near Sierra Vista, AZ). Overland flow from both sub-watersheds has short duration and happens only in response to the rainfall. Vegetation on the grassland sub-watershed includes 3- to 6-m-tall mesquite (Prosopis velutina), at about 10-m spacing, with approximately plentiful intercanopy desert grass till 1-m tall. Vegetation varies from mainly grass in the northern reaches to the mesquite in the southern reaches and is seasonally dormant.

Since this research investigates use of NDVI in an IUH model, the La Terraza watershed, consisting of two different land use sub-watersheds was selected. The urban sub-watershed would be approximately of constant NDVI but the grassland one might have some changes during different seasons. As regards, most rainfall–runoff events occur in summer monsoon in this area, the grassland sub-watershed might not have many changes during the summer as well. Therefore, it would be possible to assign an average NDVI for each sub-watershed for the study period. Accordingly, this watershed was selected due to satisfying the requirements to achieve the research goal.

2.2. Field measurements

Stream stages measurements at 1-min intervals, made by an installed gauge upstream of a 90° v-notch weir at the concrete channel conjoining two sub-watersheds (Station 1, USGS Station 09470820) and at the outlet of the combined sub-watersheds (Station 2, USGS Station 09470825), are available from May 2005 until September 2008. Stage data were transformed to discharge using a standard v-notch weir rating (Rantz, 1983). Sediment loads trapped behind the weirs were removed regularly and did not affect the stages. Rainfall data were collected by the USDA-Agricultural Research Service's Southwest Watershed Research Center (SWRC) at 1-min intervals at six rain gauges from 2005 to 2008 (SWRC Gauges 401, 402, 403, 404, 420 and 424) (USDA, 2013). Both sub-watersheds are ephemeral and all runoff is the result of precipitation events with no baseflow. The average rainfall of all of rain gauges was considered as the input rainfall on both sub-watersheds. Using the ϕ-index method (Chow et al., 1988), the excess hyetograph of each event was extracted from observed hyetographs. In this way, any rainfall prior to the beginning of direct runoff was taken as initial abstraction. Since the study area is small, the rainfall distribution was assumed uniform over the whole watershed. In this study 12 storm events occurring in both sub-watersheds (during 2005–2008) were selected to examine the proposed model's performance.

2.3. Satellite imagery

Remote sensing provides a helpful tool for precise detection of land cover changes over time and over relatively large areas. The effect of land cover change on the proposed geomorphologic rainfall–runoff model was explored using Landsat TM images, as well as rainfall and runoff data. A well-developed global archive of Landsat images is available, and is widely used to detect and monitor the land-cover changes (Kepner et al., 2008). The Landsat TM data with a 30 m spatial resolution were used to detect land uses variation. The TM satellite images of the studied area (on path 35, row 38) were downloaded from the USGS website (https://earthexplorer.usgs.gov/login/). Since for the study area the majority of rainfall–runoff events occur during June till September, images taken in these four months over the years 2005–2008 were used to detect the land cover changes. As the urban sub-watershed is of approximately constant land cover, also the grassland land cover might not have many changes during these four months of year (June till September); the average of Vegetation Index for the selected images could be assigned for each sub-watershed. Cloud-free conditions over the watershed should be regarded for

the image selection. Seven images were available with mentioned condition over the years 2005–2008 in June till September.

3. Methodology

In this research, we used remote sensing and GIS tools to characterize the land cover changes of the sub-watersheds of the La Terraza watershed, and to investigate their impacts on the proposed geomorphologic IUH model. A description of remote sensing analysis and developed hydrologic model is presented below.

3.1. Remote sensing analysis

The large scale monitoring and detecting the land cover degradation can be provided using satellite remote sensing data (Eklundh and Olsson, 2003). Following Li et al. (2015), Landsat TM images were processed using ENVI imagery analysis software (ENVI, 2009a) to define the vegetation cover. Seven cloud-free TM satellite images were used to detect the land cover changes of the study area (Fig. 2) and pre-processing was applied to the images to produce the land cover map. This section describes the image pre-processing procedure and the concept of NDVI.

3.1.1. Image pre-processing

The image pre-processing performed in this study includes image preparation, and geometric, radiometric and atmospheric corrections as described briefly below.

(i) Image preparation

Landsat 4–5 images consist of seven spectral bands. Layer stacking was used to create a multiband file from geo-referenced images with different cell sizes, extents, and projections (ENVI, 2009b). The input bands were resampled and re-projected to a common output projection and cell (pixel) size. This output includes a geographic extent that either contains all of the input file extents or only the data extent where all of the files overlap. Then, the watershed boundary was used to subset the stacked layer via ROIs (region of interests) operation. In this way, the study area could be extracted from the whole image.

(ii) Geometric correction

The purpose of geometric image correction is to eliminate geometric distortions caused by different factors that differ for each image acquisition event to ensure every picture cell is located in its true planimetric map location (Sriwongsiatnon et al., 2011). The selected images in this study were all geo-referenced to the same co-ordinate system without any need to conduct further geometric correction.

(iii) Radiometric correction

The images were also pre-processed by radiometric modification. This correction transforms the image data obtained by different sensors into a common radiometric scale and decreases signal variations uncorrelated to the brightness of the image surface, such as spectral radiance and top of atmospheric (TOA) reflectance (Sriwongsiatnon and Taesombat, 2011). After application of radiometric correction, images taken on different dates by several sensors could be compared (Sriwongsiatnon et al., 2011). TM imagery provides the spectral information in the format of a Digital Number (DN). Using DN values, spectral radiance (L) in $\mathrm{W\,m^{-2}\,sr^{-1}\,\mu m^{-1}}$ can be computed via the following equation (Sriwongsiatnon et al., 2011):

$$L = G(DN) + B \tag{1}$$

where G is the band-specific rescaling gain factor and B is the band specific rescaling bias factor. To better evaluation of the images, the variability between sensors should be reduced. In this way, the spectral radiance (L) (obtained by Eq. (1)) was transformed to a planetary or exoatmospheric reflectance via Eq. (2). This procedure eliminates the cosine effects. The cosine effects are resulted from different acquisition times and compensate for different values of the exoatmospheric solar radiances due to the variations of the spectral bands (Chander and Markham, 2003),

$$R^* = \frac{\pi d^2 L}{E_0 \cos\theta_z} \tag{2}$$

where R^* is the TOA reflectance (dimensionless), d is the earth–sun distance in astronomical units, E_0 is the mean solar exoatmospheric spectral irradiance, and θ_z is the solar zenith angle (degrees). The relation between the earth–sun distance (d) and the Julian day (Dy) of the satellite data acquisition can be expressed as (Sriwongsiatnon and Taesombat, 2011):

$$d = 1 - [0.01672\cos(0.9856(Dy - 4))] \tag{3}$$

(iv) Atmospheric correction

There is a remarkable interaction between the radiation of the earth surface and atmosphere prior to arrival of radiation to the satellite sensor. Such interaction is much significant when the target surface includes non-bright objects (e.g., water or vegetation). The purpose of atmospheric correction is to eliminate the atmospheric effects to specify true surface reflectance values and to determine physical characteristics of the Earth's surface. The Darkest Pixel (DP) method as a reliable method for visible, near-infrared and short-wave-infrared spectral areas can be applied for land cover and vegetation monitoring in local level (Hadjimitsis et al., 2010). The DP atmospheric correction method was employed to pre-process the images in the current study.

3.1.2. Normalized Difference Vegetation Index (NDVI)

The seven processed satellite images were used to calculate the NDVI values for the study area.

NDVI measures the photosynthetic activity indirectly and varies between −1 for low and +1 for high photosynthetic activity. The NDVI as a well-known Vegetation Index introduced by Rouse et al. (1974) as:

$$NDVI = \frac{\rho_{NIR} - \rho_{RED}}{\rho_{NIR} + \rho_{RED}} \tag{4}$$

The main concept behind the NDVI is that for vegetated surface, red (ρ_{RED}) and near-infrared (ρ_{NIR}) wavelengths are characterized by high and low absorptions, respectively (Chen et al., 2003). Chlorophyll reflects about 20% in the red (ρ_{RED}) and 60% in the near-infrared (ρ_{NIR}). The contrast among the responses of these bands is the quantified absorbed energy by chlorophyll which indicates level of different vegetation lands (Tucker and Sellers, 1986).

The NDVI value for a specific pixel always varies from −1 to +1; and the NDVI value of a pixel with no green leaves will be close to zero. Water bodies are specified by extreme negative values, surfaces with no vegetation cover result in zero NDVIs, and the highest density of green leaves is indicated by NDVI value close to +1 (0.8–0.9). NDVI is related to the leaf area index (LAI) and vegetation coverage; the higher the NDVI, the larger the LAI, and the higher the vegetation coverage. Therefore, NDVI indicates the vegetation cover level and also acts as a beneficial index for monitoring vegetation variations and land cover changes.

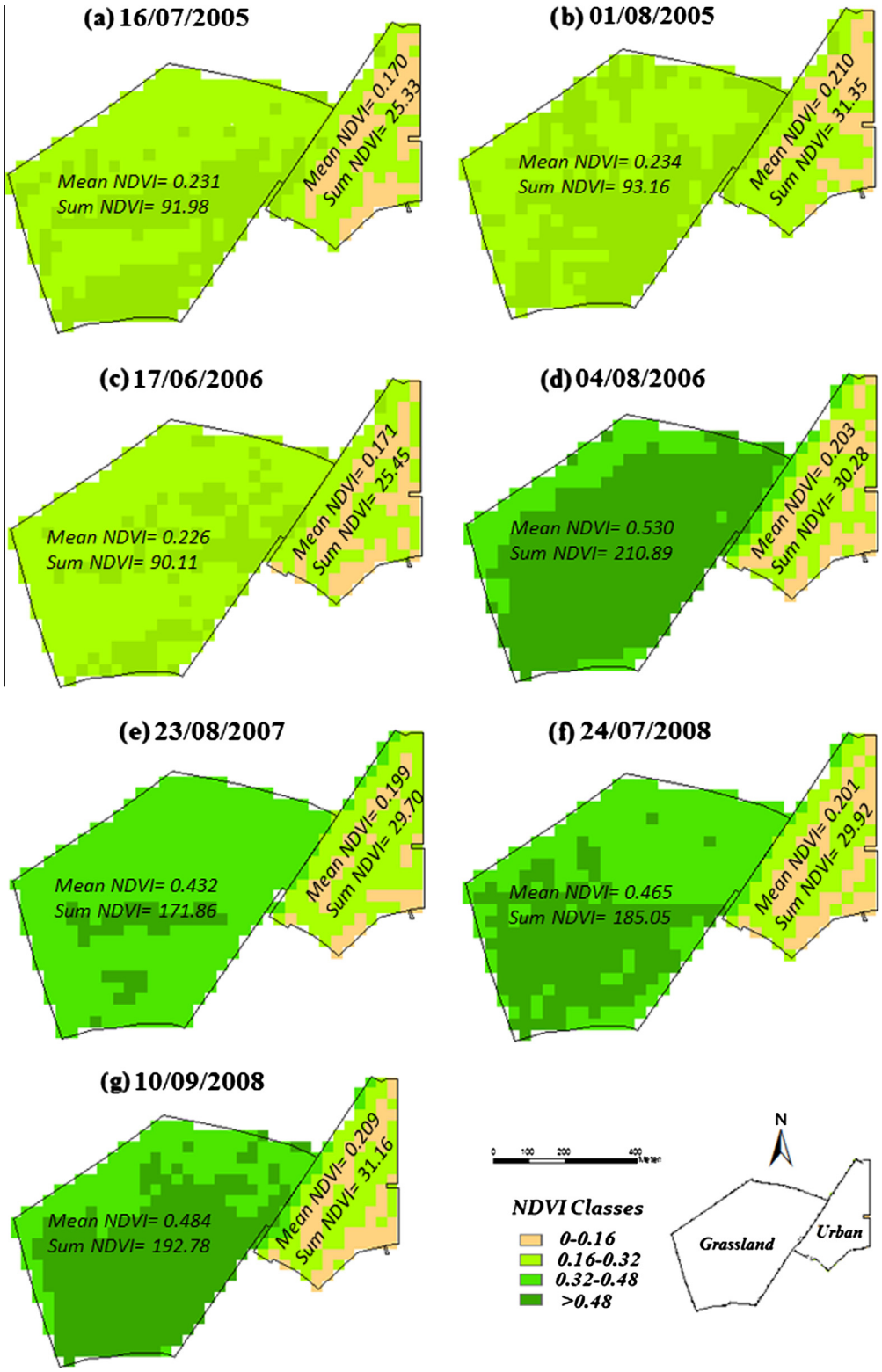

Fig. 2. NDVI classification map of Landsat TM images for seven dates.

The aforementioned steps were applied to obtain the NDVI maps of the study area for seven images. Fig. 2 shows processed Landsat images of the study area. The NDVI classification in Fig. 2 describes the spatial land cover of two sub-watersheds. The NDVI values which are smaller than 0.16, present the urbanized part of the watershed, while the higher NDVI values show the higher vegetation coverage. The mean NDVI values range from 0.170 to 0.210 in the urbanized sub-watershed, and from 0.226 to 0.530 in the grassland sub-watershed.

The NDVI properties of the processed images are also presented in Fig. 2. The 'Sum NDVI' values indicate the summation of NDVIs in all pixels of each sub-watershed land cover map. The NDVI of

each sub-watershed was calculated using ENVI and GIS tools. The summation of NDVIs (over all pixels) in each sub-watershed was calculated as:

$$NDVI_w = \sum_{i=1}^{l} NDVI_i \tag{5}$$

where $NDVI_w$ is the summation of NDVI (Sum NDVI) of the sub-watershed, and l is the number of pixels in each sub-watershed's image.

The average of Mean NDVI values for all seven images in grassland and urban sub-watersheds are respectively 0.372 and 0.195 and 147.98 and 29.03 for Sum NDVI.

As it can be seen from the images (Fig. 2), the NDVI range of variation is relatively small (as expected) during the four-month study period for the urban sub-watershed. However, some changes are observed in the grassland sub-watershed during the study period.

In the southern part of the grassland sub-watershed (which is covered mostly by mesquite) the NDVI has larger values in all images, while the upper part (which is covered by grass and changes monthly during the growing phenology) has smaller NDVI values. The largest changes are observed in the upper part of the grassland sub-watershed which is dominant by desert grasses which respond and grow rapidly with summer rainfall. These changes occur during different months also from year-to-year (see Fig. 2). Overall, there is an increasing trend from the years 2005 to 2008 in the processed images. Similar results were also found in monthly variation; in general, the NDVI values are increasing from June to early September. The minimum and maximum NDVIs are predominantly observed at June and August, respectively in both sub-watersheds (see Fig. 2).

3.2. Geomorphological Cascade of Unequal linear Reservoirs (GCUR)

3.2.1. Model formulation

The modeling approach of this study is based on Geomorphological Unit Hydrograph and cascade of linear Reservoirs. In this approach, a watershed is divided into sub-watersheds, and then each sub-watershed is represented by a linear reservoir. In most conceptual reservoir modeling approaches (e.g., Agirre et al., 2005; Cheng and Wang, 2002; López et al., 2012), it has been assumed that the entire watershed has the same land use and, based on the uniform land uses, the effective rainfall is divided proportionally between sub-watersheds according to the areas. Therefore, in watersheds including various land uses, although such models can lead to acceptable performance at watershed's outlet, it may lead to unsatisfactory results at outlets of interior sub-watersheds.

To overcome this problem, the changes in land cover were incorporated in the model by introducing a coefficient related to the average NDVI of each sub-watershed. This coefficient enables us to account for land use change and thereby improve the reproduction of observed hydrographs at all sub-watershed outlets. A schematic design of the GCUR model is presented in Fig. 3.

Distributing excess rainfall in proportion to sub-watershed areas; the IUH vector is calculated as (Singh, 1988):

$$[h(t)] = \frac{1}{[k]} e^{t[a]} [C] \tag{6}$$

where:

$$[C] = \begin{bmatrix} C_1 \\ C_2 \\ \cdot \\ \cdot \\ C_N \end{bmatrix}, [k] = \begin{bmatrix} k_1 \\ k_2 \\ \cdot \\ \cdot \\ k_N \end{bmatrix}, a = \begin{bmatrix} -a_1 & 0 & 0 & \dots & 0 \\ a_1 & -a_2 & 0 & \dots & 0 \\ 0 & a_2 & -a_3 & \dots & 0 \\ 0 & 0 & 0 & \dots & 0 \\ \dots & \dots & \dots & \dots & \dots \\ 0 & 0 & 0 & -a_{N-1} & -a_N \end{bmatrix} \tag{7}$$

Eq. (6) gives the IUH of each sub-watershed ($h_i(t)$) and consequently the related outflow hydrograph can be computed. Using this semi-distributed GCUR model, it is possible to incorporate hydrological conditions as well as the land use properties of the interior watershed parts. One can obtain the IUH of GCUR through (Nourani et al., 2009):

$$h_i(t) = \sum_{i=1}^{N} \frac{\frac{C_i}{A}\delta(t)}{\prod_{j=1}^{i}(k_j D + 1)} \tag{8}$$

In the original form of cascade of unequal linear reservoirs (Singh, 1988), the storage parameter (mean residence time) of each sub-watershed (k_i), represented by a reservoir, should be estimated by calibration. However, in GCUR, k_i can be linked to the geomorphological and land use properties of each sub-watershed and unknown parameter ($\bar{k}$) as:

$$k_i = \bar{k}(K_i) I_{VC_i}^{-1} \tag{9}$$

in which (Nourani et al., 2009):

$$K_i = L_i^{-0.1}\, C_i^{0.3}\, S_{0i}^{-0.3} \tag{10}$$

$\bar{k}$ is the model parameter with dimension [$TL^{-1/2}$]. I_{VC} is the calculated vegetation cover coefficient using the average NDVI obtained through remote sensing data for each sub-watershed. S_{0i} is the average overland slope, C_i is ith sub-watershed area and L, with dimension [L], is the longest flow path in the drainage network. The method of moments can be used for determining parameter $\bar{k}$ as (Nourani et al., 2009):

$$\bar{k} = \frac{M_1(Q) - M_1(I)}{\sum_{i=1}^{N}\left(\frac{C_i}{A}\sum_{j=1}^{i} K_i\right)} \tag{11}$$

Eq. (11) shows that the model parameter, $\bar{k}$, is explicitly linked to geomorphological properties of the sub-watersheds. In modeling via GCUR, only one parameter (i.e., k_i) is computed by the experimental equation (Eq. (9)) which is related to geomorphological properties (via K_i) and land-cover properties (via I_{vc}) of the sub-watersheds.

The semi-distributed GCUR model reflects the hydrological conditions of the interior parts of the watershed. In typical conceptual approaches, the entire watershed is assumed to have a uniform land use (which may lead to poor outcomes in watersheds with a variety of land uses), the GCUR approach, incorporates a coefficient related to the NDVI of each sub-watershed. The mean residence time of each sub-watershed in the GCUR model is thereby related to both the geomorphological properties and the land uses (via NDVI) and is different for each sub-watershed. Accordingly, the GCUR model incorporates the land use properties of sub-watersheds into the parameter formulation, while most of other geomorphologic models (e.g., Agirre et al., 2005; Chaoqun et al. (2008); Huang et al., 2008; Nourani et al., 2009; Cheng and Wang, 2002; López et al., 2012) consider only geomorphologic properties such as area, slope and length of watershed.

3.2.2. Formulations investigated

To examine the capability of the proposed model, three different formulations of modeling were considered.

(i) Formulation 1

In the first formulation, the entire watershed is considered as having approximately uniform land use. The geomorphologic parameters ($\bar{k}$, K_i, k_i) are calculated using watershed outlet hydrographs and geomorphological properties of the sub-watersheds (using Eqs. 9–11). This is a special case of the GCUR model, in

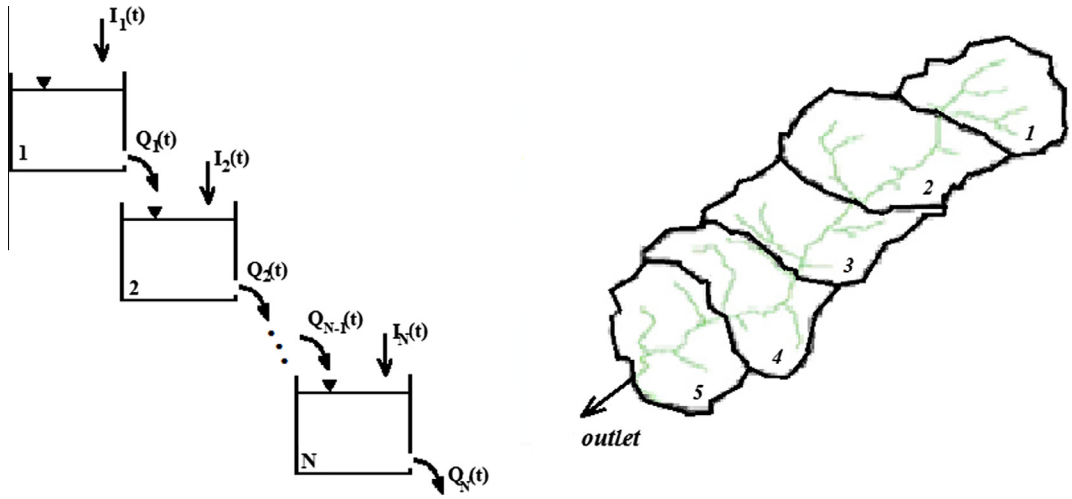

Fig. 3. A schematic of GCUR model.

which the I_{VC} parameter is equal to one and set to be the same in all sub-watersheds. As such, this formulation is similar to other geomorphologic unit hydrograph modeling approaches in which land use variation is not considered (e.g., Agirre et al., 2005; Nourani et al., 2009; López et al., 2012). The advantage of this formulation is that watershed outlet hydrographs (Eq. (8)) can be estimated using only one parameter (k_i) which, in turn, can be calculated using physical properties (L_i, C_i, S_{0i}) of the watershed. Although this model is expected to predict the outlet hydrograph accurately, it is unable to estimate the interior hydrographs reasonably when substantial land cover or land use is present. To overcome this problem and obtain accurate simulations of the interior sub-watersheds hydrographs, formulations 2 and 3 are also proposed and investigated.

(ii) Formulation 2

In the second formulation, the real time interior sub-watershed hydrograph can be estimated using the available effective rainfall hyetograph and corresponding outlet hydrograph.

In this situation, the parameters ($\bar{k}$, K_i, I_{VCi}, k_i) are estimated for each event considering geomorphologic and vegetation cover parameters obtained using GIS tools and remote sensing data using Eqs. (9)–(11) for each sub-watershed. Since the physical and land use properties of sub-watersheds can be different, this formulation considers such differences and provides the interior sub-watersheds hydrographs with reasonable accuracy. In fact, with an available data set consisting of effective rainfall hyetographs ($I(t)$), watershed's outlet hydrograph (here, $Q_2(t)$) and physical properties of sub-watershed, obtained using remote sensing data, the interior sub-watershed hydrograph (here, $Q_1(t)$) can be estimated accurately. However, it should be noted that while this formulation is able to estimate the real time interior sub-watershed discharge, it is not capable of forecasting future floods. Through this formulation the interior sub-watershed discharge is estimated based on the outlet's hydrograph at the same time.

(iii) Formulation 3

In this formulation, some of the available observed historical rainfall hyetographs over the watershed and hydrographs at the watershed's outlet are used to calibrate the model to use for estimation of hydrographs at both the watershed outlet and the interior sub-watersheds for probable rainfall over the watershed in future. For this, some observed events from the past are used to calibrate and verify the model. First, the model parameter ($\bar{k}$) is calculated using physical properties of sub-watersheds (using Eqs. (10) and (11)) for each rainfall–runoff event data set and then the average value of calculated $\bar{k}$ s from different calibration events is considered as the model parameter for verification events. In this case, both the watershed outlet hydrograph ($Q_2(t)$) and the interior sub-watershed hydrograph ($Q_1(t)$) can be forecast with adequate precision by employing the observed historical data of some events at watershed's outlet and the geomorphologic parameters and land uses of each sub-watershed using remote sensing data.

A schematic diagram of the methodology and the model input and output for the three aforementioned formulations is illustrated in Fig. 4. In all three cases the input data to the model is spatially uniform rainfall ($I(t)$) and the outlet's hydrographs ($Q_2(t)$). Since the study area is small, the rainfall is considered uniform over the whole watershed; however, as discussed above, the model approach does not limit the use of distributed rainfall over the watershed. The model is used to estimate the interior watershed's hydrographs ($Q_1(t)$) for the three formulations. In formulation 1 uniform land use is assumed for the whole watershed while in formulations 2 and 3 the land use variation is incorporated into the model via I_{VC}. Formulation 2 estimates the interior watershed's hydrographs based on outlet's hydrographs at the same time; and the formulation 3 estimates both the outlet and interior watershed's hydrographs after calibrating the model parameter ($\bar{k}$) based on the available historical events.

4. Model performance measures

The Root Mean Square Error (RMSE) and the Nash–Sutcliffe efficiency (NSE, Nash and Sutcliffe, 1970), are two model performance measures for evaluation of the hydro-environmental models (Gupta et al., 2009). To assess the performance of the proposed model, both of these criteria are reported. According to Legates and McCabe (1999) a hydrological model can be adequately evaluated by NSE and RMSE, but owing to the importance of the peak discharge in flood control and the volume of runoff in water resources management, two other important criteria, the ratio of absolute error of peak flow (E_P) and the ratio of absolute error of hydrograph's volume (E_V) were also used in this study to evaluate the proposed methodology as (Rwasoka et al., 2014):

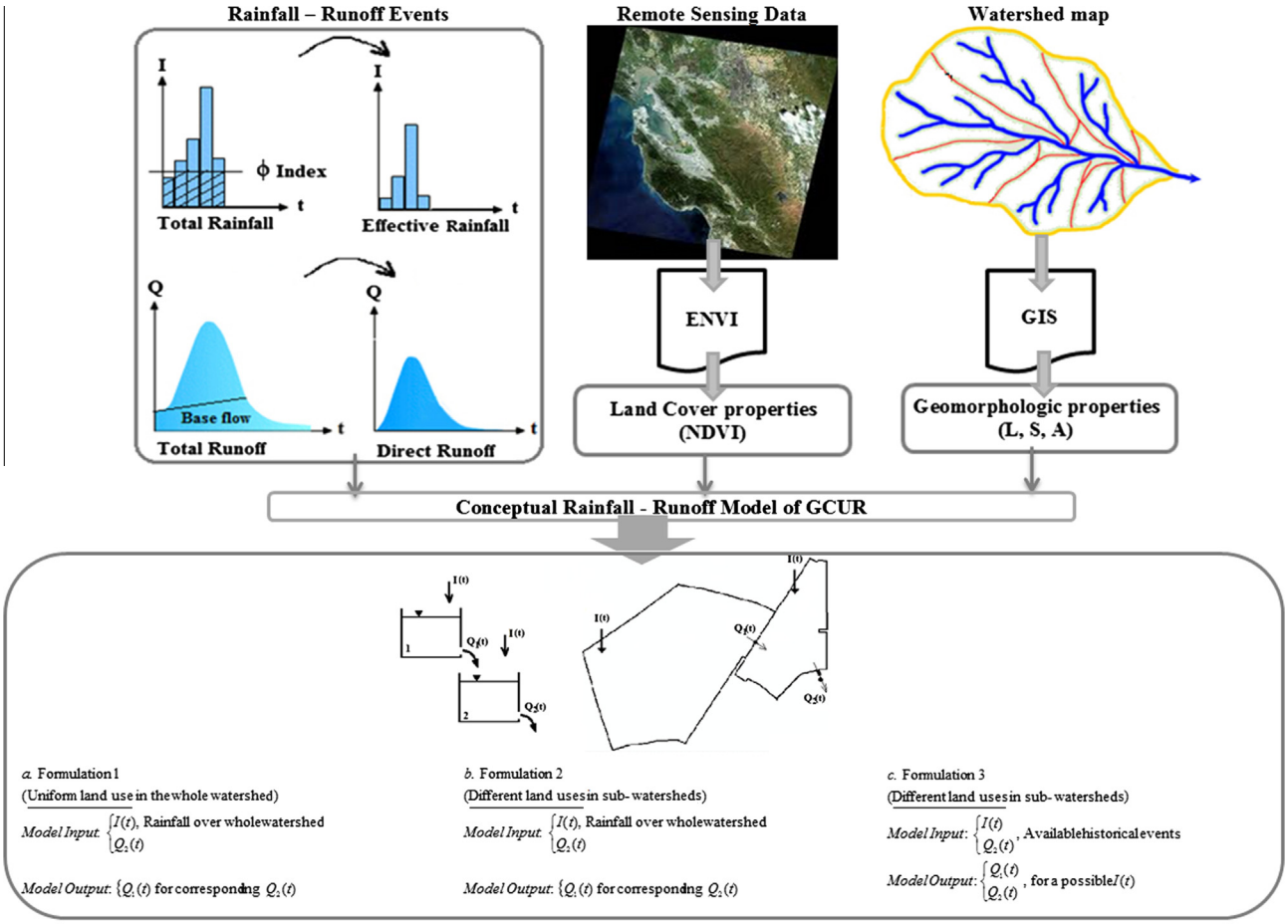

Fig. 4. A schematic of proposed methodology via three formulations.

$$NSE = 1 - \frac{\sum_{t=1}^{n}[Q_{t,Obs} - Q_{t,sim}]^2}{\sum_{t=1}^{n}[Q_{t,Obs} - \overline{Q_{Obs}}]^2} \tag{12}$$

$$RMSE = \sqrt{\frac{\sum_{t=1}^{n}[Q_{t,Obs} - Q_{t,sim}]^2}{n}} \tag{13}$$

$$E_P = \frac{|Q_{P,Sim} - Q_{P,Obs}|}{Q_{P,Obs}} \times 100 \tag{14}$$

$$E_V = \frac{|V_{Sim} - V_{Obs}|}{V_{Obs}} \times 100 \tag{15}$$

where $Q_{t,Obs}$ and $Q_{t,Sim}$ are the observed and computed discharges at time t; n is the number of observed data; $Q_{P,Obs}$ and $Q_{P,Sim}$ are observed and simulated peak discharges; V_{Obs} and V_{Sim} are observed and simulated volumes of hydrographs, respectively. High values for *NSE* and small values for *RMSE*, E_P and E_V indicate that the model is highly efficient.

5. Results and discussion

To evaluate performance of the proposed modeling approach, 12 storm events occurring over both sub-watersheds were selected.

Geomorphological factors for the sub-watersheds extracted by GIS and the model parameters are shown in Table 1.

Land cover detection for the study area was performed using seven images of Landsat 4–5 TM over the period 2005–2008. The NDVI of each sub-watershed was calculated using ENVI and GIS tools (Fig. 2).

The ratio of average greenness between sub-watersheds could be calculated considering the $NDVI_w$ (Eq. (5)) of each sub-watershed by averaging the value of $NDVI_w$ in seven processed images. Due to higher NDVI values, which means more pervious area in grassland sub-watershed, the contribution of effective area in runoff generation in the urban and grassland sub-watersheds are not equal and should be determined using land cover properties. These contributions could be calculated using two equations: first, the summation of the effective area of sub-watersheds participating in runoff generation is equal to the area of the whole watershed; second, the average greenness (and hence pervious area) of the grassland watershed is about 5 times as much as that of the urban one (see Sum NDVI values in Fig. 2); consequently, the contribution of effective area in runoff generation in the urban sub-watershed is 5 times as much as that of the grassland one. Therefore, the I_{VC} parameter (presented in Table 1) for each sub-watershed could be calculated as:

$$\begin{cases} I_{VC1}C_1 + I_{VC2}C_2 = A \\ I_{VCd2} = 5I_{VC1} \end{cases} \Rightarrow I_{VC1} = 0.46,\ I_{VC2} = 2.32 \tag{16}$$

Model parameter ($\overline{k}$) was then determined using sub-watershed quantities (Table 1) and 12 storm events data.

Performance of the GCUR model was examined for the three formulations explained in Section 3. For all formulations, the hydrological results were evaluated based on the observed hydrographs. The results of the simulations for the formulations are presented and discussed below.

Table 1
Geomorphological factors of sub-watersheds.

Sub-watershed	C_i (m^2)	S_{0i} (%)	L_i (m)	Impermeability (%)	Elongation ratio	Shape factor	I_{VCi}	K_i
Grassland	319,700	2.43	834.64	~0	0.76	2.18	0.46	69.90
Urban	128,310	1.55	549.55	37	0.74	2.35	2.32	56.58

5.1. Evaluation of model for formulation 1

In this formulation, two sub-watersheds of the study area having different land uses were treated as though they were as sub-watersheds with uniform and identical land use. The model parameters were calculated using observed hydrographs at the watershed outlet (the weir downstream of the urban watershed – USGS stream gauge 09470825) and the geomorphological properties of the sub-watersheds (Eqs. (9)–(11)). The I_{VC} parameter was set to be the same in both sub-watersheds and equal to one. The computed hydrographs are shown in Fig. 5. Since the model uses the geomorphologic characteristics of the watershed to calculate the model parameters, these parameter values will be, to some degree, uncertain, and comparing the computed and observed hydrographs at the watershed outlet enables a qualitative assessment of that uncertainty. As can be seen in Fig. 5, although this formulation predicts the outlet hydrograph (station 2) fairly accurately, it is unable to provide reasonable estimates of the interior hydrographs (station 1). The calculated parameters for this formulation are shown in Table 2. The average values for *NSE*, *RMSE*, E_P, and E_V at the watershed outlet are 0.80, 0.042, 20.84, and 6.60, respectively. In contrast, the averages of the aforementioned criteria at grassland sub-watershed outlet (USGS stream gauge 9470820 – inner part) are 0.24, 0.009, 40.27 and 36.59, respectively. It is obvious that this formulation is unable to provide reasonable simulation for the interior sub-watershed hydrographs and, in particular, their peak values and volume are overestimated. In some formerly presented IUH models (e.g., López et al., 2005 and Nourani et al., 2009) the effects of variable land cover were not incorporated into the model formulation. Such models might appropriately predict the interior watershed hydrographs in watersheds with approximately uniform land use, but as demonstrated herein such models will be unable to accurately estimate interior sub-watersheds hydrographs in watersheds having different land uses sub-watersheds (like the watershed in this study). To address this problem formulations 2 and 3 were considered and examined.

5.2. Evaluation of model for formulation 2

This formulation aims to estimate the interior sub-watershed hydrographs (station 1) based on information provided by outlet hydrographs (station 2) and the physical properties of the sub-watersheds, including their land cover type.

In this formulation, all of the events are used to compute corresponding interior sub-watershed (grassland) hydrographs for the study area. The calculated parameters for formulation 2 are shown in the right hand portion of Table 2. The average values for *NSE*, *RMSE*, E_P, E_V for formulation 2 at outlet (station 2) are 0.81, 0.041, 28.84, 8.23, respectively. However, the averages of aforementioned criteria at the grassland sub-watershed outlet (station 1- inner part) are now improved to 0.77, 0.006, 17.80 and 13.29, respectively. Fig. 5 compares the observed and modeled hydrographs for formulations 1 and 2. As it can be seen from Fig. 5 and Table 2, this formulation is better able to simulate the internal watershed hydrographs, illustrating the need to take land use variation into consideration within the model formulation. This formulation employs outlet hydrographs to estimate the corresponding internal watershed hydrographs; however, it is unable to forecast future discharges. The formulation 3 is considered to address this issue.

5.3. Evaluation of model for formulation 3

In this formulation, the interior and outlet hydrographs were assessed using available observed event data (uniform rainfall over the watershed and hydrographs at watershed outlet), and using physical properties of the sub-watersheds with different land cover types. Eight events were selected for model calibration to the outlet hydrographs. The remaining four events were used to examine the simulated hydrographs for the outlet (station 2) and the interior (station 1) grassland sub-watershed (see Table 3). The model parameter ($\bar{k}$) was estimated for each event using the moment method and the average of the calibrated values was used for the evaluation of the model (see Fig. 6). Based on both calibration and verification results, it can be seen that the values of the criteria are reasonable. The average evaluation stage values for *NSE*, *RMSE*, E_P, E_V at the watershed outlet (station 2) are 0.75, 0.056, 37.82, 22.85, respectively. The corresponding values for average *NSE*, *RMSE*, E_P, E_V at the grassland watershed outlet (station 1) are 0.78, 0.009, 21.37, 22.18, respectively. Clearly, accounting for land cover properties in the model formulation leads to improved efficiency at the internal sub-watershed.

The second and third studied model formulations result in acceptable values for the efficiency criteria, and indicate the ability of the model to predict runoff hydrographs at both the watershed outlet (station 2) and at internal sub-watershed (station 1). Evident from an analysis of Tables 2 and 3 is the large difference in abilities of formulation 1 and formulations 2 and 3 to predict the hydrographs at the interior sub-watershed outlets. Figs. 5 and 6, show a high level of agreement with observed hydrographs for formulations 2 and 3. This can be attributed to the value added by incorporating information about land cover variation provided by NDVI.

It is also worth noting that the GCUR model formulations of 2 and 3 (Figs. 5 and 6) both are able to simulate both the rising limbs of hydrographs (which are mostly related to storm properties) and the recession limbs (which are usually related to the watershed morphology) appropriately. In general, urban runoff tends to have a sharper rising limb and higher peak values while runoffs in natural watersheds have smaller peak values and the rising limb climbs more slowly. The hydrographs in Figs. 5 and 6, show that the overall shapes of the urban sub-watershed hydrographs are similar to each other, while those for the grassland sub-watershed tend to be more different, as expected.

Simultaneous consideration of geomorphological and land cover parameters in the formulation of the proposed model provides this capability. As indicated by E_P and E_V in Tables 2 and 3, the error of peak flow and the volume of hydrographs show acceptable accuracy in both formulations 2 and 3. Based on the results in Tables 2 and 3, it can be noted that some events show high values of error of peak flows (E_P); however, both formulations result in small values of E_V that is of great importance in water resource management.

Note that, the performance values obtained for the watershed outlet were, for most events, higher than those for the internal sub-watershed outlet in both formulations, which may be due to

Table 2
Calculated parameter of model for formulations 1 and 2.

Event	Date	Formulation 1									Formulation 2								
		Outlet					Grassland				Outlet					Grassland			
		$\bar{k}$	*NSE*	*RMSE* (mm)	E_P (%)	E_V (%)	*NSE*	*RMSE* (mm)	E_P (%)	E_V (%)	$\bar{k}$	*NSE*	*RMSE* (mm)	E_P (%)	E_V (%)	*NSE*	*RMSE* (mm)	E_P (%)	E_V (%)
1	13/08/2006	3.77	0.73	0.038	20.40	18.38	0.64	0.005	9.76	31.68	2.11	0.68	0.043	47.57	19.48	0.87	0.003	9.64	5.76
2	18/08/2005	3.91	0.72	0.049	26.20	8.51	0.54	0.015	25.22	31.02	2.17	0.64	0.059	52.10	9.13	0.74	0.011	29.83	19.54
3	23/08/2005	2.51	0.84	0.039	18.38	2.02	−0.09	0.006	76.76	46.24	1.99	0.88	0.034	16.30	1.78	0.75	0.003	1.89	8.11
4	25/08/2006	3.52	0.79	0.023	15.89	1.46	0.64	0.002	18.00	41.92	2.08	0.86	0.018	14.30	1.28	0.90	0.001	21.50	17.81
5	14/07/2008	7.88	0.81	0.038	5.04	0.13	0.52	0.006	24.32	29.75	4.21	0.80	0.034	29.54	10.59	0.80	0.004	23.97	14.36
6	18/07/2008	6.35	0.58	0.087	37.81	21.14	0.39	0.010	23.32	33.77	4.06	0.60	0.089	56.10	31.90	0.71	0.007	30.19	0.51
7	19/07/2008	6.53	0.83	0.037	29.68	0.79	−0.46	0.008	37.18	64.83	5.14	0.88	0.032	28.94	0.70	0.77	0.003	23.93	10.61
8	23/07/2008	2.38	0.92	0.038	25.56	2.13	0.47	0.009	19.28	21.23	1.91	0.93	0.033	26.45	1.85	0.54	0.009	12.02	32.98
9	04/08/2007	2.92	0.90	0.014	2.00	1.88	0.49	0.002	85.57	0.54	2.35	0.92	0.013	2.51	1.73	0.79	0.001	23.16	21.88
10	07/08/2008	2.40	0.89	0.067	25.24	2.12	0.53	0.023	35.96	30.31	1.92	0.92	0.058	23.17	1.84	0.82	0.015	15.67	7.59
11	08/08/2006	3.62	0.67	0.031	21.69	18.32	−0.25	0.002	31.40	49.20	2.94	0.74	0.030	23.99	18.50	0.84	0.001	13.85	17.68
12	14/08/2008	3.96	0.74	0.061	26.83	1.28	0.54	0.022	20.30	29.05	3.19	0.81	0.056	28.63	1.10	0.69	0.018	11.97	8.45
Average			**0.78**	**0.043**	**21.23**	**6.51**	**0.33**	**0.009**	**33.92**	**34.13**		**0.80**	**0.041**	**29.13**	**8.23**	**0.77**	**0.006**	**18.14**	**13.78**

Table 3
Verification results of formulations 1 and 3.

		Event	$\bar{k}$[a]	Formulation 1				$\bar{k}$[a]	Formulation 3			
				NSE	*RMSE*	E_P (%)	E_V (%)		*NSE*	*RMSE*	E_P (%)	E_V (%)
Verification	Outlet	9	4.61	0.85	0.017	22.42	7.41	2.96	0.83	0.018	30.59	15.53
		10	4.61	0.74	0.103	37.92	33.35	2.96	0.68	0.114	45.46	38.72
		11	4.61	0.62	0.034	31.30	18.41	2.96	0.71	0.032	43.75	18.21
		12	4.61	0.75	0.060	23.35	8.66	2.96	0.79	0.059	31.46	18.95
	Average			**0.74**	**0.053**	**28.75**	**16.96**		**0.75**	**0.056**	**37.82**	**22.85**
	Grassland	9	4.61	0.81	0.001	50.10	8.78	2.96	0.84	0.001	15.08	17.37
		10	4.61	0.41	0.026	22.63	81.71	2.96	0.76	0.017	24.79	29.08
		11	4.61	0.20	0.002	14.87	12.68	2.96	0.76	0.001	21.93	35.72
		12	4.61	0.44	0.023	31.26	47.53	2.96	0.74	0.017	23.66	14.58
	Average			**0.47**	**0.013**	**29.72**	**37.68**		**0.78**	**0.009**	**21.37**	**24.18**

[a] The average of the calculated values of events 1–8.

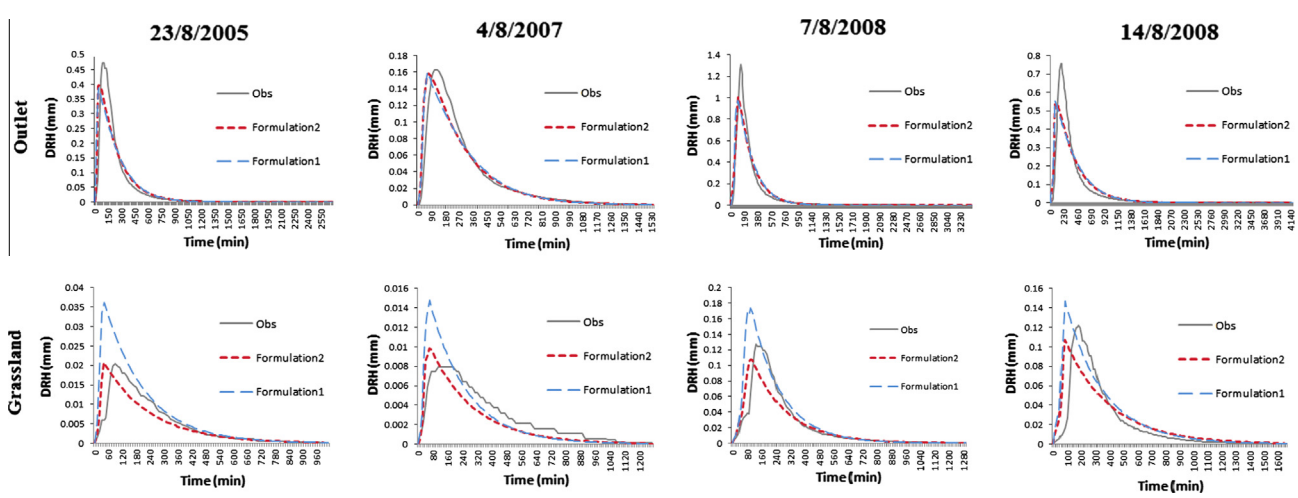

Fig. 5. Comparison of observed and calculated hydrographs obtained via formulations 1 and 2.

the use of outlet hydrographs for calculating the model parameter (Eq. (11)). Also, this might be due to less uncertainty in urban watersheds where runoff to rainfall ratios are much larger than in the natural sub-watershed. For small runoff to rainfall ratios in the natural sub-watershed the uncertainties associated with rainfall measurement errors and spatial variability can a dominant part of the overall model prediction uncertainty (high noise to signal ratio). In addition, the parameters values (i.e., physical and land cover properties) in urban sub-watershed are approximately constant while these values are more variable over time in grassland sub-watershed. This characteristic would show less uncertainty in the urban watershed which leads to more precise result at watershed outlet than that of the grassland one.

Formulation 1 has slightly better performance at watershed outlet, but it is unable to detect land cover variability in its model formulation and so to estimate the internal watershed

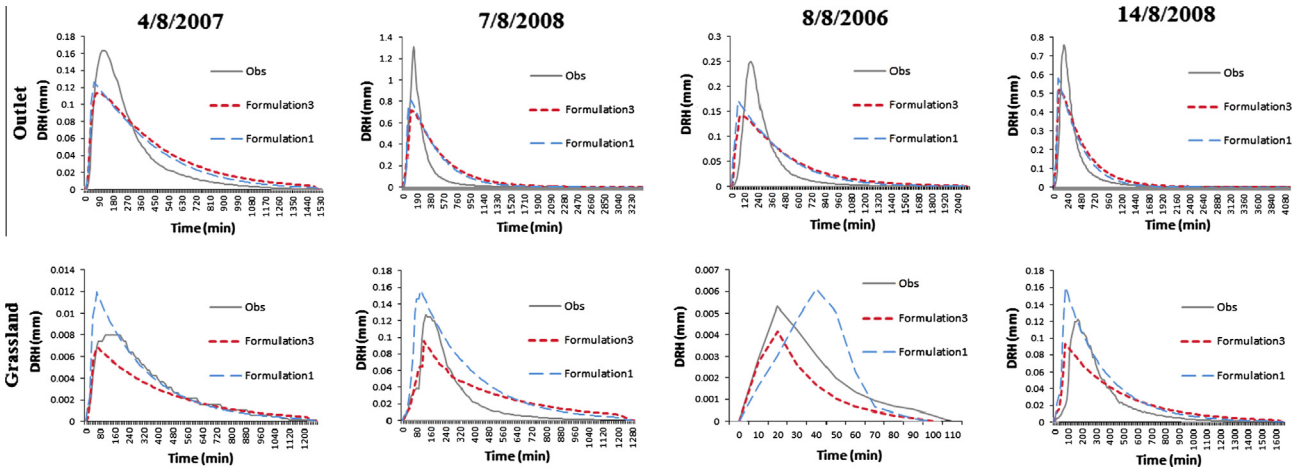

Fig. 6. Comparison of observed and calculated hydrographs obtained via formulations 1 and 3 in verification events.

hydrographs appropriately. Overall, peak discharge and runoff volume for the grassland sub-watershed was over-estimated via formulation 1. Over 40% improvement is achieved in simulated peak discharge and runoff volume at interior watershed outlet if accounting for the variability of land cover in model formulation (see averages of E_P and E_V in Tables 2 and 3).

The mean residence time of each sub-watershed represented by a linear reservoir, k_i, in the unequal cascade of linear reservoirs with distributed excess rainfall may be different from one sub-watershed to the other (Singh, 1988). Therefore, calculation of parameters is difficult and almost undeterminable due to the large number of parameters. The requirement to estimate parameters is inevitable in any conceptual and geomorphology based rainfall–runoff model (Saeidifarzad et al., 2014). As it has been proven by different studies, the problem of parameter calibration in most of hydrologic applications is nonlinear, ill posed, multimodal, and non-convex (Duan et al., 1992). However, in the presented GCUR model, there is only one parameter ($\bar{k}$). GCUR model considers not only the geomorphologic properties of the watershed, but also the land cover variation using remote sensing data and considers land use/cover changes of the sub-watershed in parameter formulation. Application of geomorphologic and land cover data from inside of watershed led to more realistic parameters which reflect the variation between watersheds with different land covers.

As discussed earlier, however, other similar geomorphologic models might be able to simulate the internal hydrographs of the watersheds with uniform land uses, but they are unable to predict hydrographs at the interior parts of the watershed with different land uses. In contrast, the presented GCUR model can also reflect the hydrological conditions of the internal parts of the watershed with divergent land uses detecting land cover changes taking advantages of remote sensing data.

Using three formulations for the GCUR model, it was demonstrated that this model provides a promising approach for simulating sub-watershed outlet hydrographs. Each presented formulation provides a specific application that can be used for different purposes. As discussed before, formulation 1 can be applied to watersheds where the land cover is approximately uniform over the sub-watersheds. Formulation 2 could be employed to estimate interior sub-watershed hydrographs utilizing effective rainfall and observed hydrographs at outlet with regards to geomorphological and land cover properties of the sub-watersheds with different land uses; and, formulation 3 can be used to estimate runoff from the outlet and internal sub-watershed hydrographs using available historical rainfall–runoff event data set and the sub-watershed's physical specifications. The combination of the geomorphological parameters with vegetation cover index in model formulation makes it suitable for prediction of watershed interior runoff.

6. Concluding remarks

The GCUR model is able to improve the efficiency of geomorphological rainfall–runoff simulations at the interior of the La Terraza watershed, located in southeastern Arizona, by taking into account land use/cover, monitored via remotely sensed data. The GCUR model as a geomorphological model has been constructed on the basis of linear reservoir concept and watershed physical properties. Consideration of land use/cover in the model leads to acceptable results at both watershed and interior sub-watershed outlets, particularly for watersheds like the studied watershed where different land uses sub-watersheds have. The overall efficiency of prediction was slightly poorer for the internal sub-watershed than for the outlet. Over 40% improvement is achieved in simulated peak discharge and runoff volume at interior watershed outlet if accounting for the variability of land cover in the model formulation. Application of three formulations of the model reveals that two formulations in which the land cover effects are considered in the model formulation are able to simulate the hydrographs at an acceptable level near the gauge locations (in a hydrological sense).

The model was applied on a watershed in semi-arid Arizona where the rainfall–runoff events are usually occurred in summer monsoon which the land cover does not change significantly from one event to another and so the NDVI can be approximately set to be constant for all events. The vegetation cover changes affect runoff response of a watershed through changing the hydrological cycle in the basin. Therefore, this model can be applied to predict runoffs for different seasons, in which the vegetation cover and so NDVI is varied due to seasonal changes. The effect of seasonal NDVI can be analyzed by hydrologists in watersheds with seasonal variety in event data to develop the geomorphological rainfall–runoff models. It is suggested to apply this model for different season's events to detect seasonal runoff variation with regards to NDVI changes.

Acknowledgments

This paper was supported by a research Grant of the University of Tabriz. Our special thanks go to Jeffrey R. Kennedy at USGS in Tucson, Arizona, who provided a useful collection of data related to the study area. Also the useful helps of Hadi Delafrouz in GCUR model programming are appreciated. We would also like

thank the University of Arizona that provided the opportunity of a research visit for the third author.

References

Agirre, U., Goñi, M., López, J.J., Gimena, F.N., 2005. Application of a unit hydrograph based on subwatershed division and comparison with Nash's instantaneous unit hydrograph. Catena 64, 321–332.

Baret, F., Guyot, G., 1991. Potentials and limits of vegetation indices for LAI and APAR assessment. Remote Sens. Environ. 35 (2–3), 161–173.

Braud, I., Vich, A.I.J., Zuluaga, J., Fornero, L., Pedrani, A., 2001. Vegetation influence on runoff and sediment yield in the Ands region: observation and modeling. J. Hydrol. 254, 124–144.

Braud, I., Breil, P., Thollet, F., Lagouy, M., Branger, F., Jacqueminet, C., Kermadi, S., Michel, K., 2013. Evidence of the impact of urbanization on the hydrological regime of a medium-sized periurban catchment in France. J. Hydrol. 485, 5–23.

Canters, F., Batelaan, O., de Voorde, T.V., Chorman ski, J., Verbeiren, B., 2011. Use of impervious surface data obtained from remote sensing in distributed hydrological modeling of urban areas. In: Yang, X. (Ed.), Urban Remote Sensing: Monitoring, Synthesis and Modeling in the Urban Environment. John Wiley & Sons, Chichester, UK, pp. 255–273.

Chander, G., Markham, B., 2003. Revised Landsat-5 TM radiometric calibration procedures and postcalibration dynamic ranges. IEEE Trans. Geosci. Remote Sens. 41 (11), 2674–2677.

Chaoqun, L., Shenglian, G., Zhang, W., Zhang, J., 2008. Use of Nash's IUH DEM's to identify the parameters of an unequal-reservoir cascade IUH model. Hydrol. Process. 22, 4073–4082.

Chen, P.Y., Srinivasan, R., Fedosejevs, G., Kiniry, J.R., 2003. Evaluating different NDVI composite techniques using NOAA-14 AVHRR data. Int. J. Remote Sens. 24 (17), 3403–3412.

Cheng, S.J., Wang, R.Y., 2002. An approach for evaluating the hydrological effects of urbanization and its application. Hydrol. Process. 16, 1403–1418.

Chormanski, J., Van de Voorde, T., De Roeck, T., Batelaan, O., Canters, F., 2008. Improving distributed runoff prediction in urbanized catchments with remote sensing based estimates of impervious surface cover. Sensors 8, 910–932.

Chow, V.T., Maidment, D.R., Mays, L.W., 1988. Applied Hydrology. McGraw-Hill, New York, USA.

de Vos, N.J., Rientjes, T.H.M., Gupta, H.V., 2010. Diagnostic evaluation of conceptual rainfall–runoff models using temporal clustering. Hydrol. Process. 24, 2840–2850.

Duan, Q., Gupta, V.K., Sorooshian, S., 1992. Effective and efficient global optimization for conceptual rainfall–runoff models. Water Resour. Res. 28, 1015–1031.

Eklundh, L., Olsson, L., 2003. Vegetation index trends for the African Sahel 1982–1999. Geophys. Res. Lett. 30 (8), 1430. http://dx.doi.org/10.1029/2002GL016772.

ENVI, 2009a. ENVI User's Guide, Version 4.7., ITT Visual Information Solutions.

ENVI, 2009b. Basic Tools, ENVI User's Guide, Version 4.7., ITT Visual Information Solutions.

Ferguson, B.K., 1998. Introduction to Storm Water. John Wiley & Sons Inc, U.S., 255p.

Goodrich, D.C., Woolhiser, D.A., 1991. Catchment Hydrology. Rev. Geophys. 29, 202–209.

Goodrich, D.C., Keefer, T.O., Unkrich, C.L., Nichols, M.H., Osborn, H.B., Stone, J.J., Smith, J.R., 2008. Long-term precipitation database, Walnut Gulch experimental Watershed, Arizona, United States. Water Resour. Res. 44, W05S04. http://dx.doi.org/10.1029/2006WR005782.

Gupta, H.V., Kling, H., Yilmaz, K.K., Martinez, G.F., 2009. Decomposition of the mean squared error and NSE performance criteria: implications for improving hydrological modeling. J. Hydrol. 377, 80–91.

Hadjimitsis, D.G., Papadavid, G., Agapiou, A., Themistocleous, K., Hadjimitsis, M.G., Retalis, A., Michaelides, S., Chrysoulakis, N., Toulios, L., Clayton, C.R.I., 2010. Atmospheric correction for satellite remotely sensed data intended for agricultural applications: impact on vegetation indices. Nat. Hazards Earth Syst. Sci. 10, 89–95.

Hawley, R.J., Bledsoe, B.P., 2011. How do flow peaks and durations change in suburbanizing semi-arid watersheds? a southern California case study. J. Hydrol. 405, 69–82.

Hollis, G.E., 1975. The effect of urbanization on floods of different recurrence interval. Water Resour. Res. 11, 431–435.

Huang, H.J., Cheng, S.J., Wen, J.C., Lee, J.H., 2008. Effect of growing watershed imperviousness on hydrograph parameters and peak discharge. Hydrol. Process. 22, 2075–2085.

Jones, J.A., Grant, G.E., 1996. Peak flow responses to clear-cutting and roads in small and large basins, western Cascades, Oregon. Water Resour. Res. 32 (4), 959–974.

Kang, I.S., Park, J.I., Singh, V.P., 1998. Effect of urbanization on runoff characteristics of the On-Cheon stream watershed in Pusan, Korea. Hydrol. Process. 12, 351–363.

Kennedy, J.R., Goodrich, D.C., Unkrich, C.L., 2013. Using the KINEROS2 modeling framework to evaluate the increase in storm runoff from residential development in a semiarid environment. J. Hydrol. Eng. 18, 698–706.

Kepner, W.G., Semmens, D.J., Hernandez, M., Goodrich, D.C., 2008. Evaluating hydrological response to forecasted land use change. The North America Land Cover Summit. Association of American Geographers, Washington, DC, pp. 275–292.

Legates, D.R., McCabe Jr., G.J., 1999. Evaluating the use of "goodness-of-fit" measures in hydrologic and hydro-climatic model validation. Water Resour. Res. 35 (1), 233–241.

Li, W., Saphores, L.D.M., Gillespie, T.W., 2015. A comparison of the economic benefits of urban green spaces estimated with NDVI and with high-resolution land cover data. Landscape Urban Plan. 133, 105–117.

López, J.J., Gimena, F.N., Goñi, M., Agirre, U., 2005. Analysis of a unit hydrograph model based on watershed geomorphology represented as a cascade of reservoirs. Agric. Water Manage. 77 (1–3), 128–143.

López, J.J., Gimena, F.N., Giraldez, J.V., Ayuso, J.L., Goni, M., 2012. Comparative analysis of a geomorphology-based instantaneous unit hydrograph in small mountainous watersheds. Hydrol. Process. 26, 2909–2924.

Ma, M., Frank, V., 2006. Interannual variability of vegetation cover in the Chinese Heihe River Basin and its relation to meteorological parameters. Int. J. Remote Sens. 27 (16), 3473–3486.

McGulloch, J.S.G., Robinson, M., 1993. History of forest hydrology. J. Hydrol. 150, 189– 16..

Miller, S.N., Kepner, W.G., Mehaffey, M.H., Hernandez, M., Miller, R.C., Goodrich, D.C., Kim Devonald, F., Heggem, D.T., Miller, W.P., 2002. Integrated landscape assessment and hydrologic modeling for land cover change analysis. J. Am. Water Resour. As. 38 (4), 915–929.

Miller, S.N., Semmens, D., Goodrich, D., Hernandez, M., Miller, R., Kepner, W., Guertin, D.P., 2007. The automated geospatial watershed assessment tool. Environ. Modell. Softw. 22, 365–377.

Nash, J.E., 1957. The form of the instantaneous unit hydrograph. Hydrol. Sci. Bull. 3, 114–121.

Nash, J.E., Sutcliffe, J.V., 1970. River flow forecasting through conceptual models I: a discussion of principles. J. Hydrol. 10 (3), 282–290.

Nourani, V., Mano, A., 2007. Semi-distributed flood runoff model at the sub-continental scale for southwestern Iran. Hydrol. Process. 21 (23), 3173–3180.

Nourani, V., Singh, V.P., Delafrouz, H., 2009. Three geomorphological rainfall–runoff models based on the linear reservoir concept. Catena 76, 206–214.

Pickup, G., 1995. A simple model for predicting herbage production from rainfall in rangelands and its calibration using remotely sensed data. J. Arid Environ. 30, 227–245.

Qi, J., Marsett, R.C., Moran, M.S., Goodrich, D.C., Heilman, P., Kerr, Y.H., Dedieu, G., Chehbouni, A., Zhang, X.X., 2000. Spatial and temporal dynamics of vegetation in the San Pedro River basin area. Agric. Forest Meteorol. 105, 55–68.

Rantz, S.E., 1983. Measurement and computation of stream flow. I: Measurement of stage and discharge, Water Supply Paper 2175, USGS, Reston, VA.

Rodriguez-Iturbe, I., Valdes, J.B., 1979. The geomorphologic structure of the hydrologic response. Water Resour. Res. 15 (6), 1409–1420.

Rouse, J.W., Haas, R.H., Schell, J.A., Deering, D.W., Harlan, J.C., 1974. Monitoring the vernal advancements and retrogradation (green wave effect) of nature vegetation. NASA/GSFC Final Report, Greenbelt.

Rwasoka, D.T., Madamombe, C.E., Gumindoga, W., Kabobah, A.T., 2014. Calibration, validation, parameter identifiability and uncertainty analysis of a 2 – parameter parsimonious monthly rainfall-runoff model in two catchments in Zimbabwe. Phys. Chem. Earth. 67, 36–46.

Saeidifarzad, B., Nourani, V., Aalami, M.T., Chau, K.-W., 2014. Multi-site calibration of linear reservoir based geomorphologic rainfall–runoff Models. Water 6, 2690–2716.

Sriwongsiatnon, N., Surakit, K., Thianpopirug, S., 2011. Influence of atmospheric correction and number of sampling points on the accuracy of water clarity assessment using remote sensing application. J. Hydrol. 401, 203–220.

Sriwongsiatnon, N., Taesombat, W., 2011. Effects of land cover on runoff coefficient. J. Hydrol. 410, 226–238.

Simmons, D.L., Reynolds, R.J., 1982. Effects of urbanization on base flow of selected south-shore streams, Long Island, New York. J. Am. Water Resour. Assoc. 18, 797–805.

Singh, V.P., 1988. Hydrologic systems. Rainfall-Runoff Modeling. Prentice-Hall, Englewood Cliffs, vol. I.

Sun, R., Gao, X., Liu, C.-M., Li, X.-W., 2004. Evapotranspiration estimation in the Yellow River Basin, China using integrated NDVI data. Int. J. Remote Sens. 25 (13), 2523–2534.

Tucker, C.J., Townshend, J.R.G., Goff, T.E., 1985. African land-cover classification using satellite data. Science 227, 369–375.

Tucker, C.J., Sellers, P.J., 1986. Satellite remote sensing of primary vegetation. Int. J. Remote Sens. 7, 1395–1416.

Udelhoven, T., Stellmes, M., Del Barrio, G., Hill, J., 2009. Assessment of rainfall and NDVI anomalies in Spain (1989–999) using distributed lag models. Int. J. Remote Sens. 30 (8), 1961–1976.

U.S. Dept. of Agriculture (USDA), 2013. Southwest Watershed Research Center online data access. <http://tucson.ars.ag.gov/dap>.

Wang, J., Rich, P.M., Price, K.P., 2003. Temporal responses of NDVI to precipitation and temperature in the central Great Plains, USA. Int. J. Remote Sens. 24, 2345–2364.

Wang, J., Ishidaira, H., Xu, Z.X., 2012. Effects of climate change and human activities on inflow into the Hoabinh Reservoir in the Red River basin. Proc. Environ. Sci. 13, 1688–1698.